



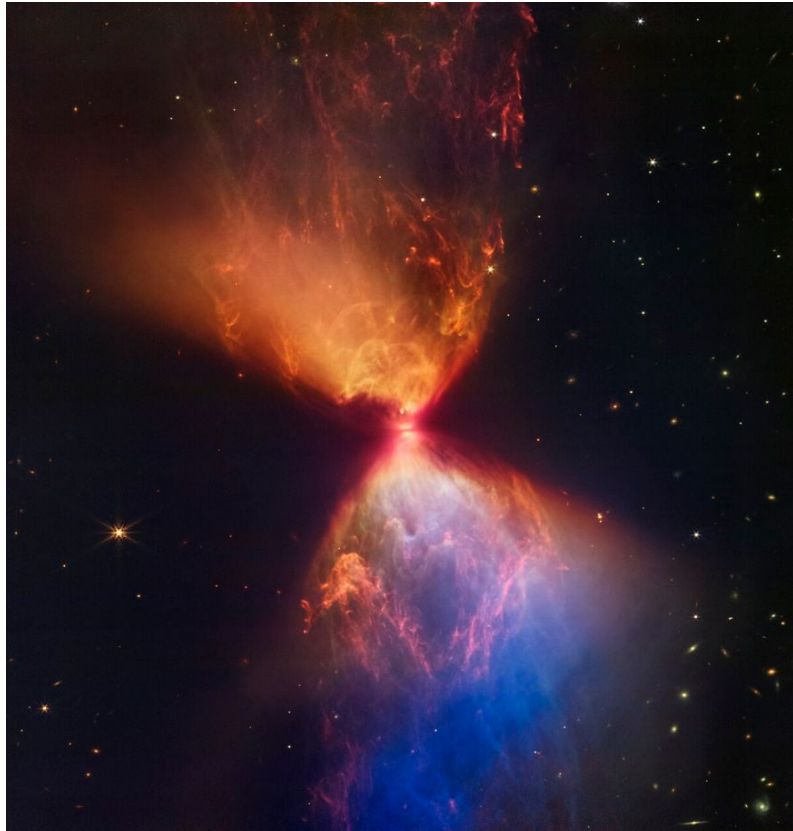
An IRAM 3 mm spectral survey of the Class 0/I protostar L1527: evidence for limited reprocessing before disc scales

H. T'KINDT¹, S. Maret¹, R. Le Gal^{1,2}

1: Université Grenoble Alpes, CNRS, IPAG, F-38000 Grenoble, France

2: IRAM, 300 rue de la piscine, F-38406 Saint-Martin d'Hères, France

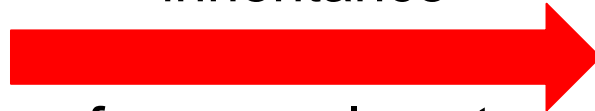
➤ Context : Protostellar formation



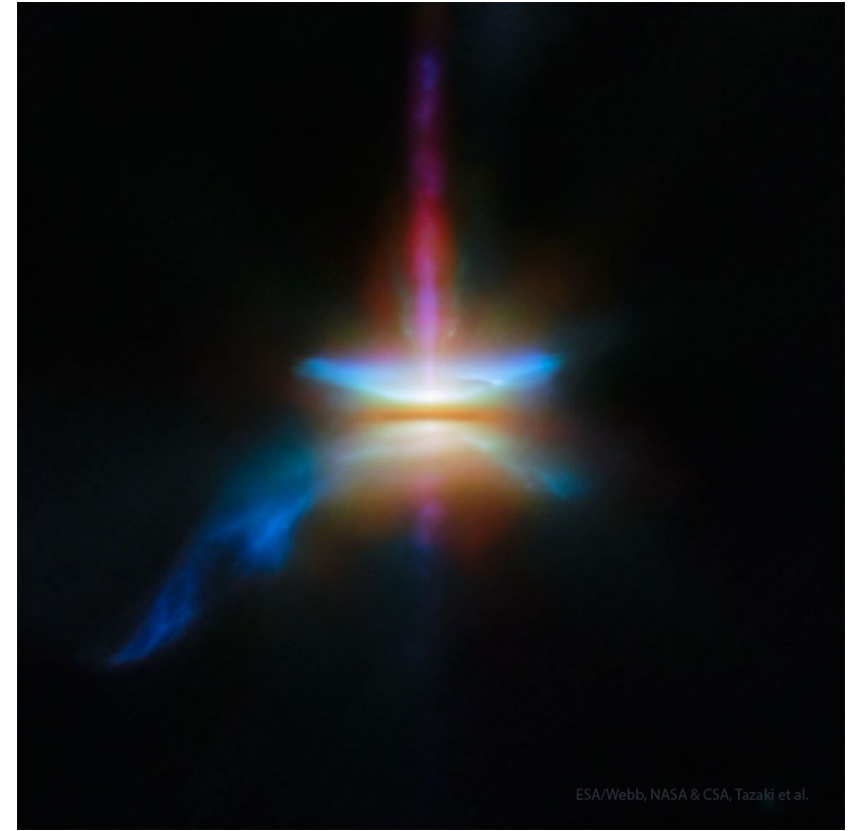
L1527 with its envelope and protostellar disk

NASA, ESA, CSA and STScI, J. DePasquale (STScI)

Is there some chemical inheritance



from envelope to protoplanetary disks ?



Protoplanetary disk of HH30

[James Webb Space Telescope](#), [ESA](#), [NASA](#) & [CSA](#), [R. Tazaki et al.](#)

➤ Context : L1527

Located in the Taurus at 140pc from Earth

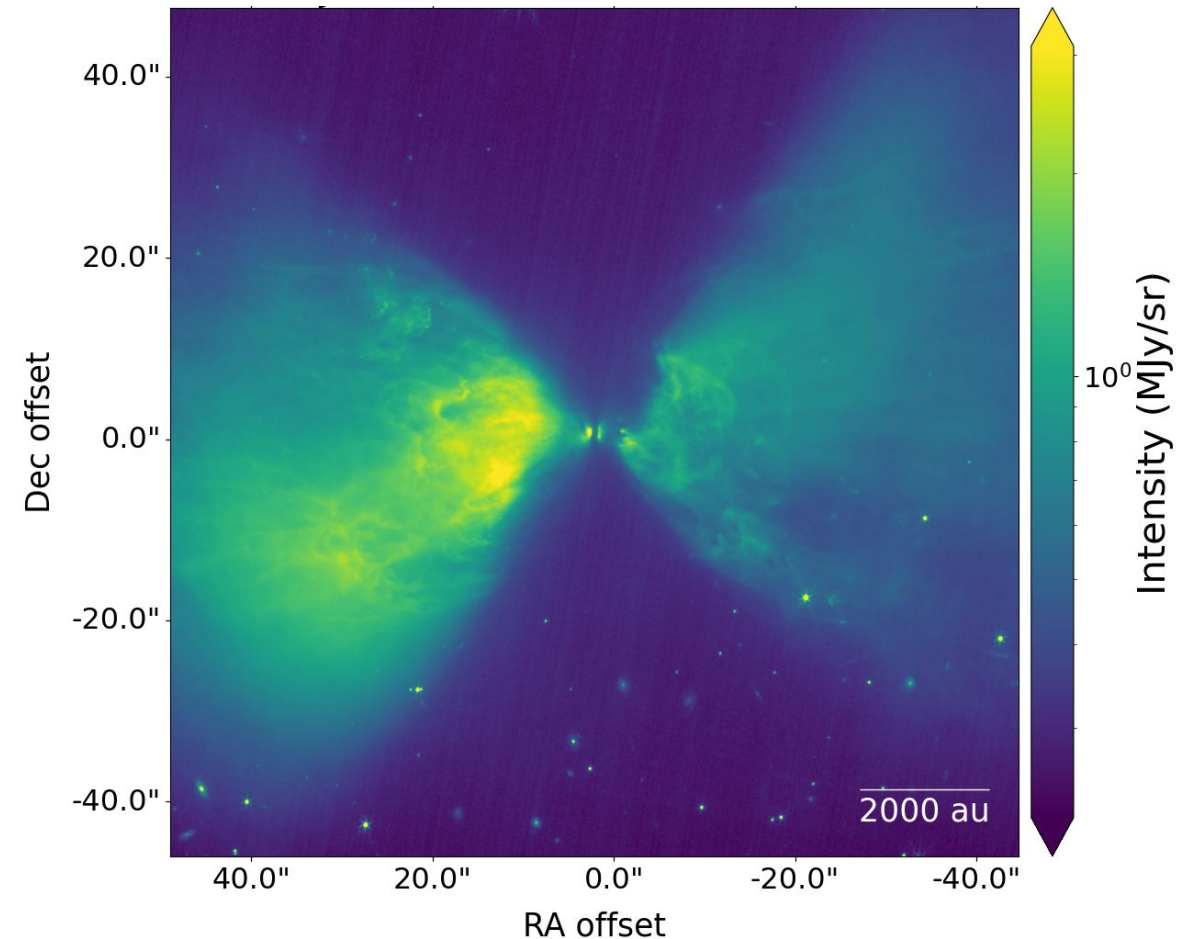
Class 0/I protostar

Embedded in its natal environment

Has an almost edge-on disk (EoD)

- Seen from North to South in JWST image

Considered to be a Warm Carbon Chain Chemistry (WCCC) source



JWST NIRCам observation of the 3.3 μm continuum emission in L1527. The map has been cropped to the same as the ones done with NOEMA and the IRAM 30m

➤ Context : Aims and observations

Usage of 3mm observations :

- From NOEMA radio interferometer
- From IRAM 30m single dish
- Studying a region of 90''x90''

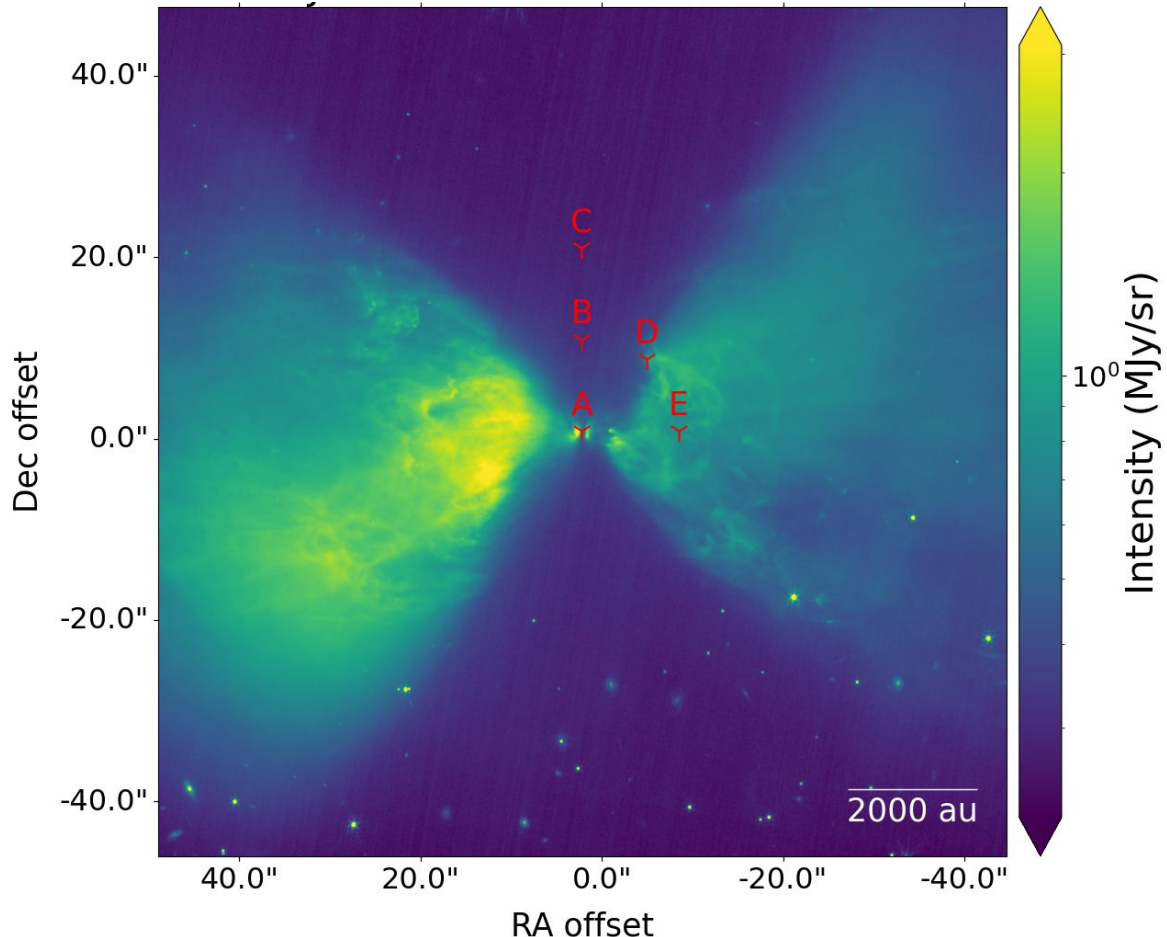
Many molecules are seen :

- 213 transitions
- 71 species

Aims :

- Characterise the chemical composition of young protoplanetary disks
- See the impact of the infalling envelope

LTE line fitting at key positions



JWST NIRCcam observation of the 3.3 μm continuum emission in L1527. Red markers show the studied positions

Molecule	A	B	C	D	E
^{13}CO	✓	✓	✓	✓	⊙
C^{18}O	✓	✓	✓	✓	⊙
HCO^+	✓	✓	✓	⊙	⊙
DCO^+	✓	✓	✓	✓	✓
H^{13}CO^+	✓	✓	✓	✓	✓
HC^{18}O^+	✓	✓	✓	✓	✓
H_2CO	✓	✓	✓	⊙	✓
C_2H	✓	✓	✓	✓	✓
C_2D	✓	✓	✗	✓	✓
C_3H	✓	✓	✗	✓	✓
C_4H	✓	✓	✓	✓	✓
ortho c - C_3H_2	✓	✓	✓	✓	✓
para c - C_3H_2	✓	✓	✓	✓	✓
ortho l - C_3H_2	✓	✓	✗	✗	✗
para l - C_3H_2	✓	✓	✗	✗	✗
ortho l - C_4H_2	✓	✓	✗	✗	✗
para l - C_4H_2	✓	✓	✗	✗	✗
N_2H^+	✓	✓	✓	✓	✓
HC_3N	✓	✓	⊙	⊙	⊙
DC_3N	✓	✓	✓	✗	✗
HC_5N	✓	✓	✗	✓	✓
HCN	⊙	⊙	⊙	✓	✓
DCN	✓	✓	✓	✓	✓
H^{13}CN	✓	✓	✓	✓	✓
HC^{15}N	✓	✓	✗	✓	✗
HNC	✓	✓	✓	✓	⊙
DNC	✓	✓	✓	✓	✓
HN^{13}C	✓	✓	✓	✓	✓
H^{15}NC	✓	✓	✓	✓	✓
SO	✓	✓	✓	✓	✓
CS	✓	✓	✓	⊙	⊙
C^{34}S	✓	✓	✗	✓	✓
C_2S	✓	✓	✗	✓	✓
Number of molecules	33	33	23	28	27

Table of the molecules modeled with an LTE model using MCMC algorithm at the five targeted positions

Green check = Successful model

Red cross = Failure of the MCMC (lack of SNR)

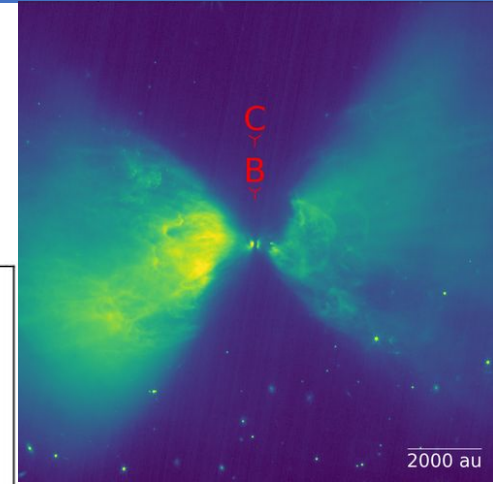
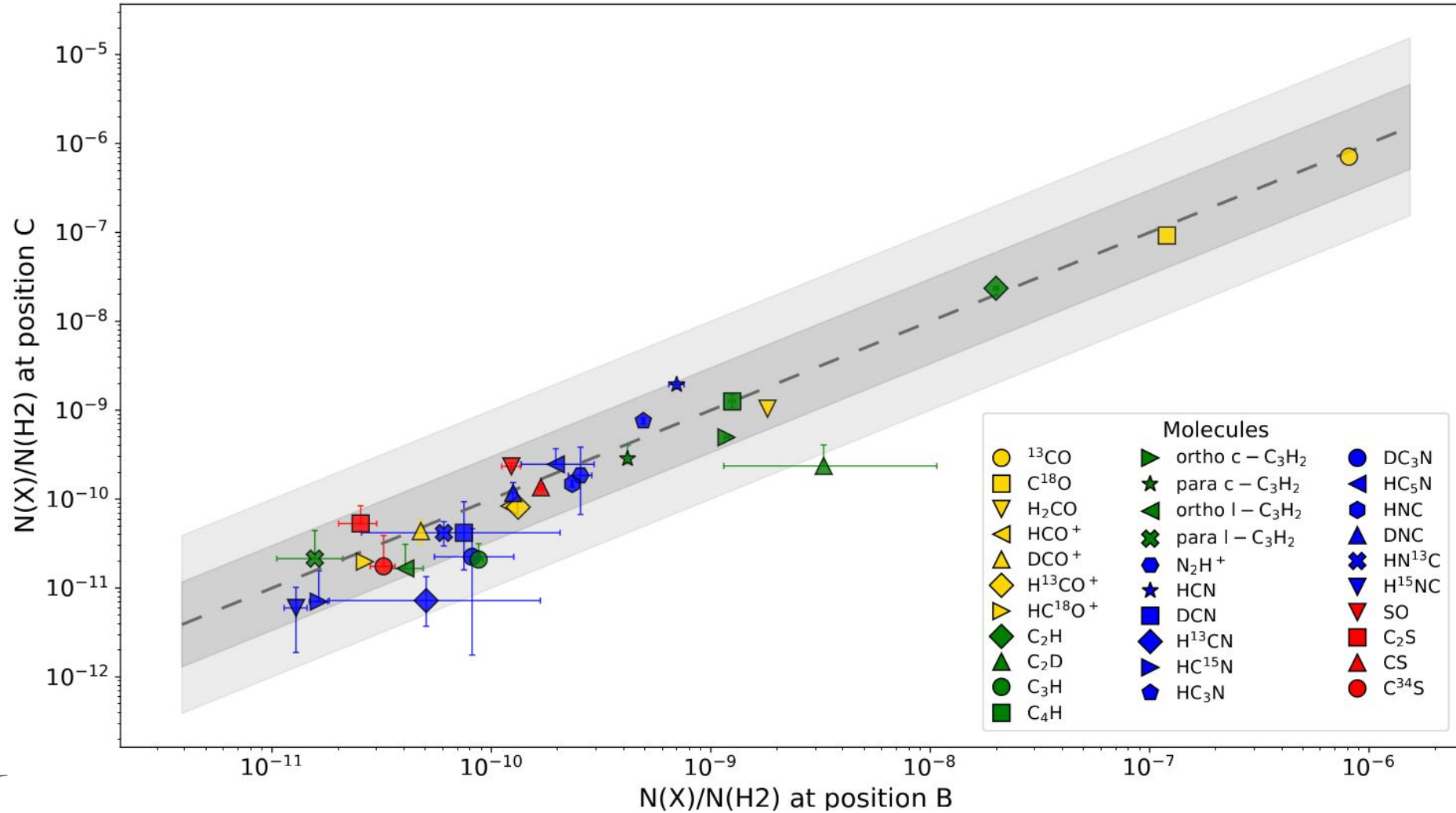
Orange circled mark = Converged MCMC BUT results have to be taken with caution (opacity effects, two velocity components, non gaussian line, etc)

Table from T'Kindt et al. (in prep.) →

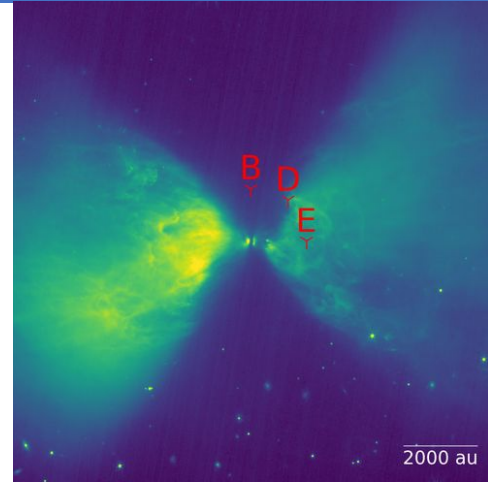


Comparison of the abundances

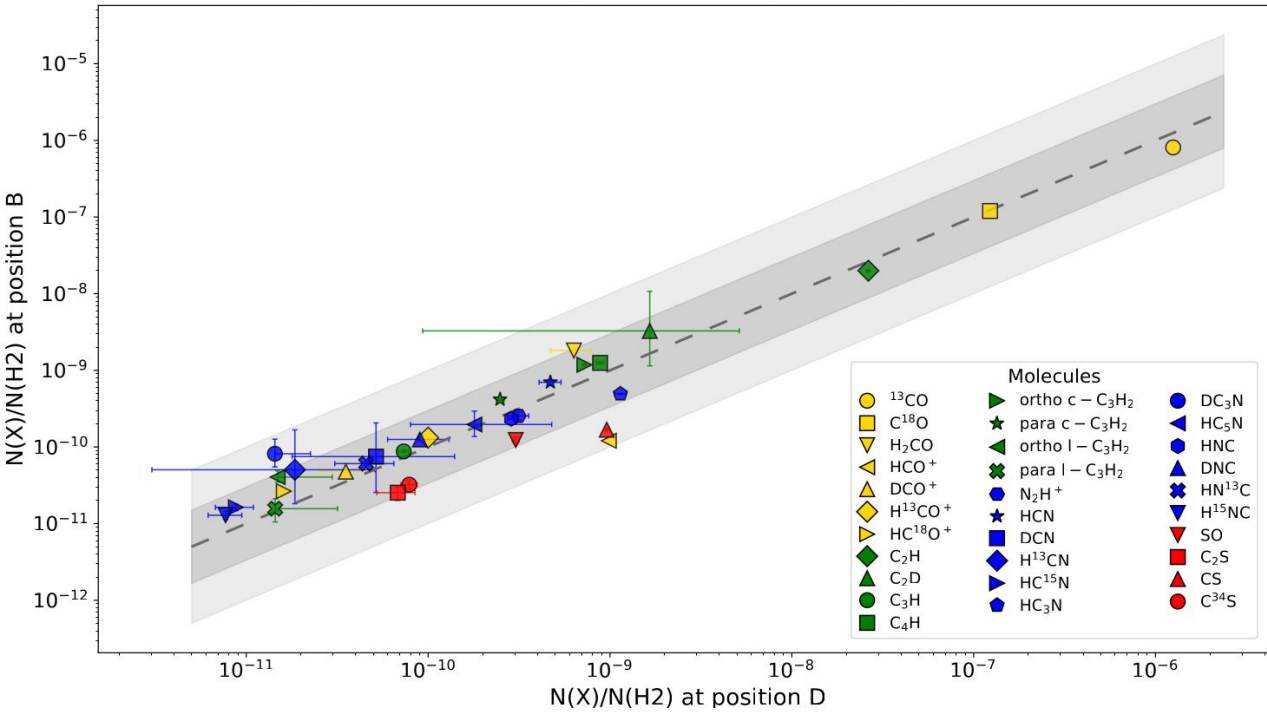
Envelope-axis comparison: positions B and C



Comparison of the abundances

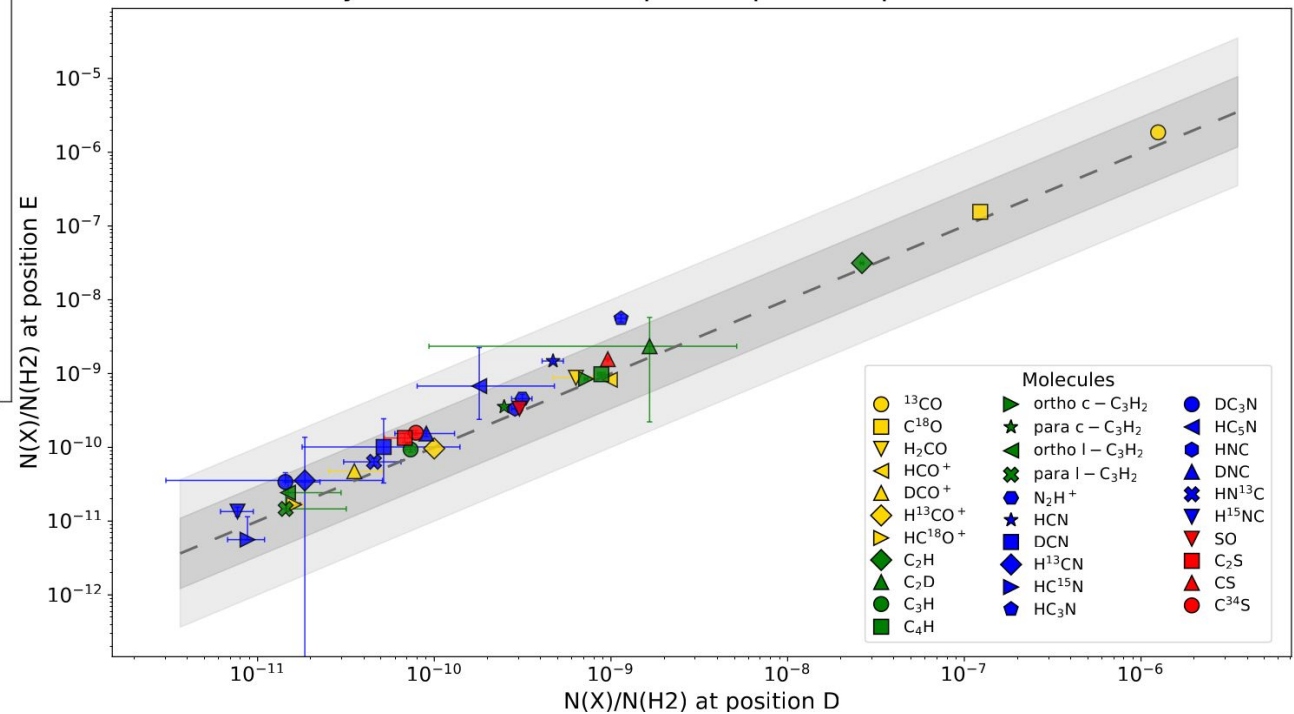


Cavity-wall versus cavity-center comparison: positions D and B



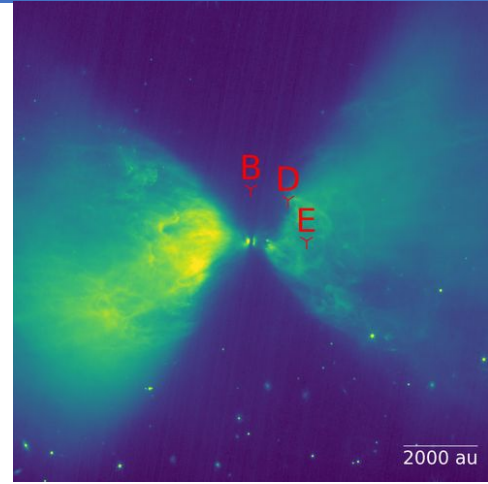
T'Kindt et al. (in prep.)

Cavity-wall versus envelope comparison: positions D and E

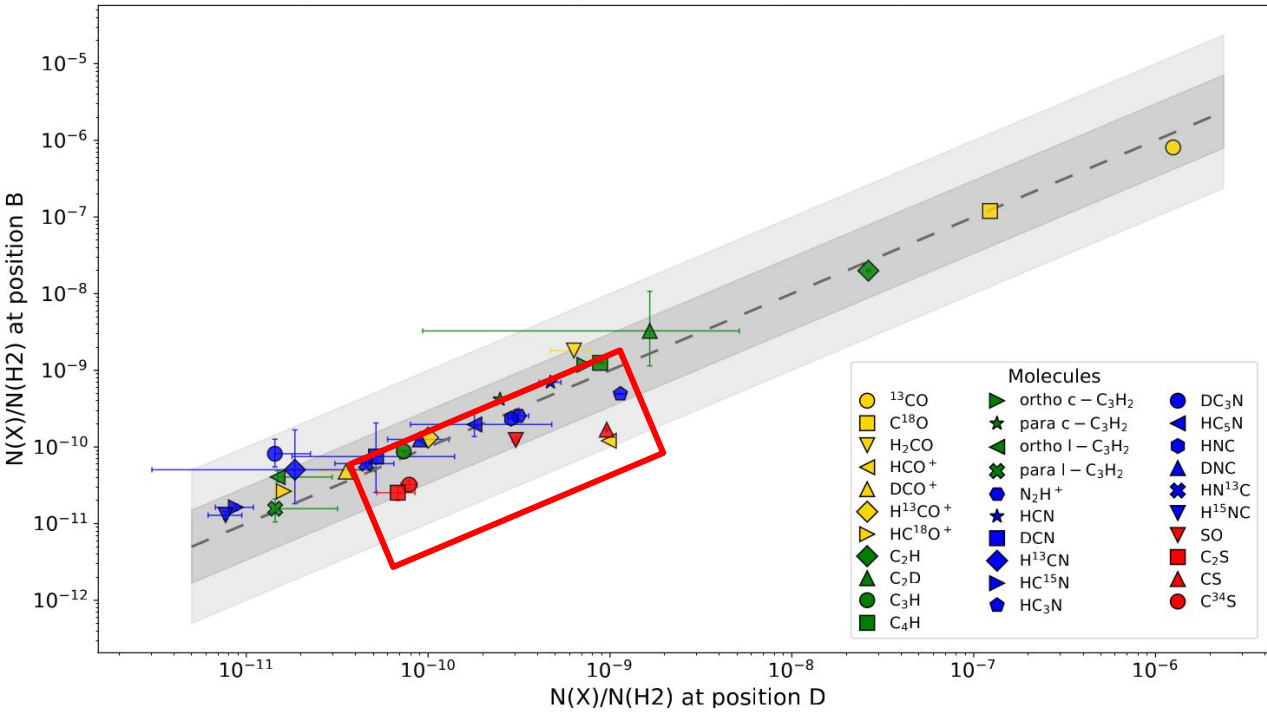


T'Kindt et al. (in prep.)

Comparison of the abundances

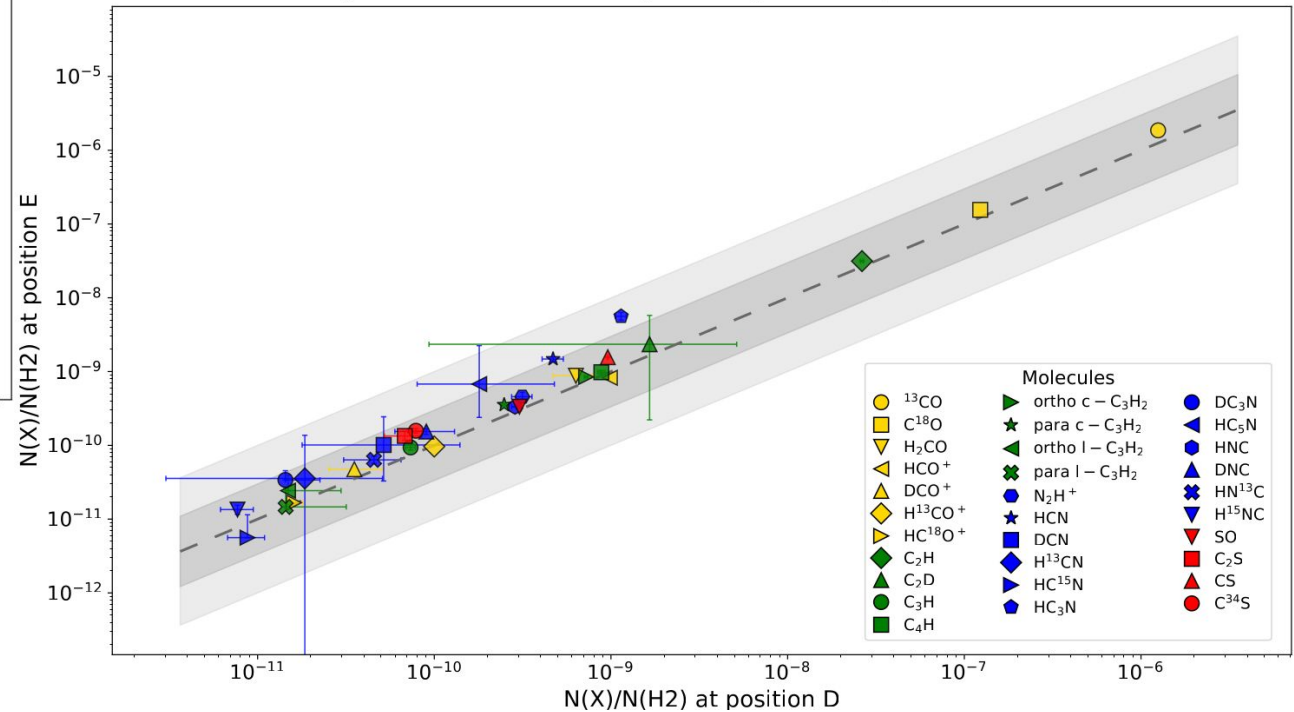


Cavity-wall versus cavity-center comparison: positions D and B



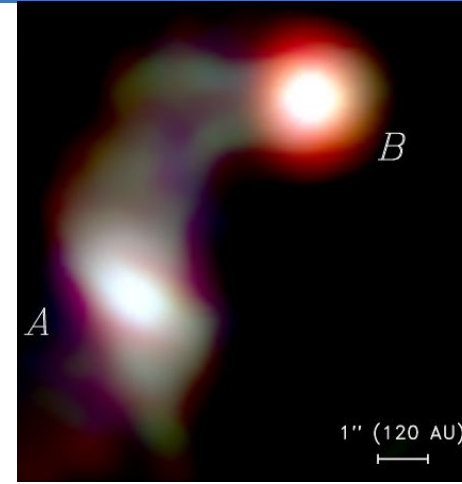
T'Kindt et al. (in prep.)

Cavity-wall versus envelope comparison: positions D and E



T'Kindt et al. (in prep.)

➤ L1527 vs IRAS 16293 B



Abundances (w.r.t. C18O) in IRAS 16293 B taken from the work of the “ALMA Protostellar Interferometric Line Survey” (PILS) collaboration :

- Jørgensen, J. K., Van Der Wiel, M. H. D., Coutens, A., et al. 2016, A&A, 595, A117

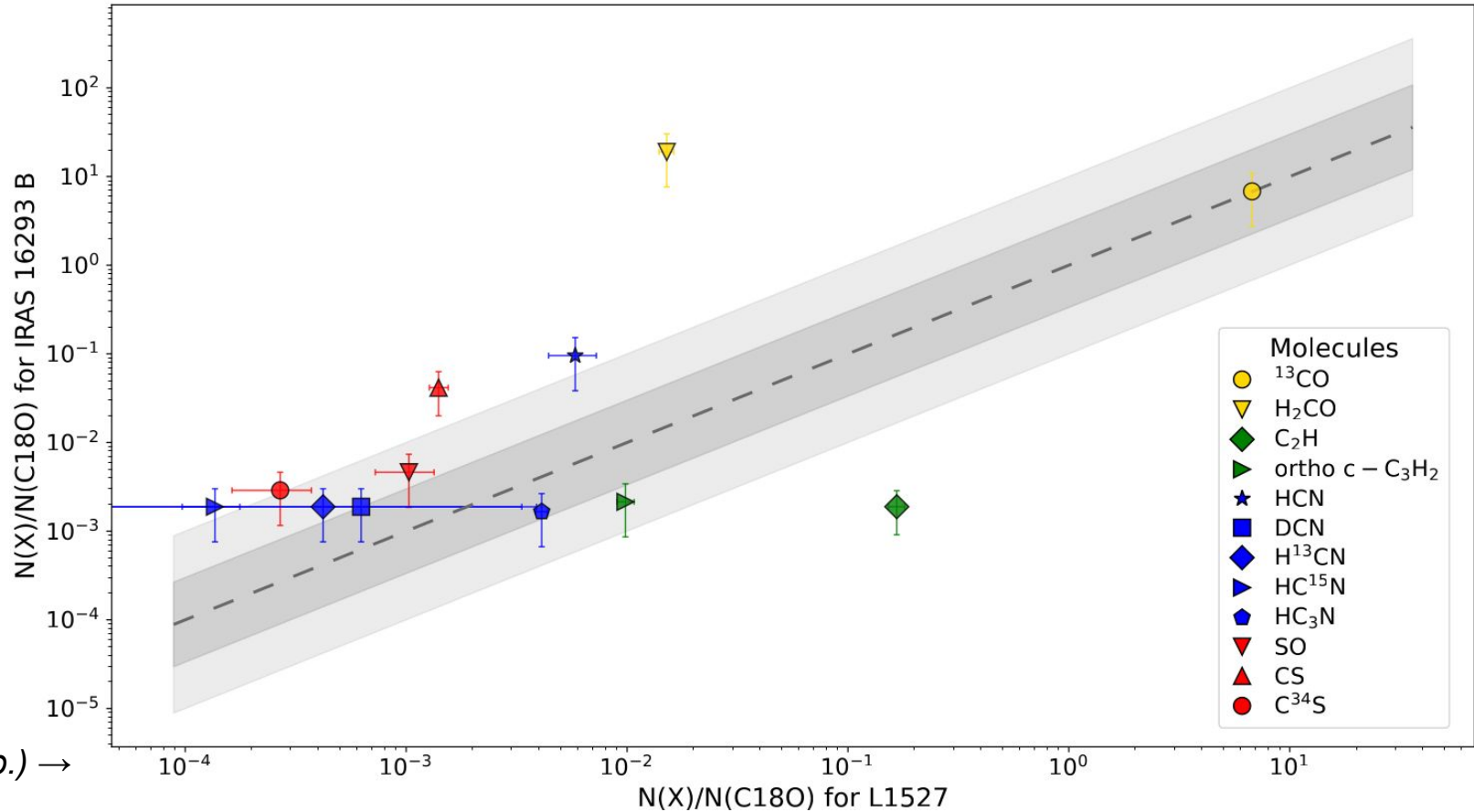
Comparison of abundances in L1527 and IRAS 16293 B

IRAS 16293 B :

- Rho Oph. at 160pc
- Embedded Class 0
- Hot corino

Lots of Complex Organic Molecules (COMs) are detected in IRAS 16293 B but not in L1527

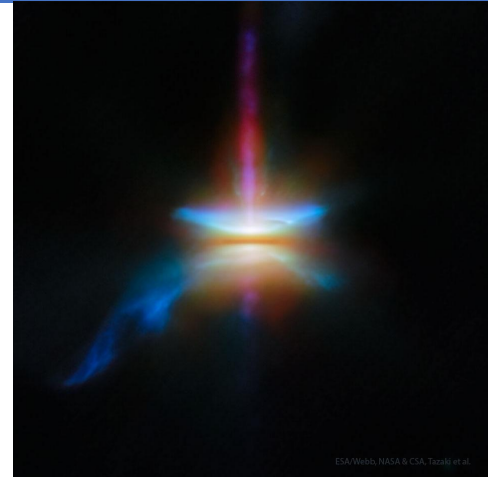
More carbon chains detected in L1527 than in IRAS 16293 B



T'Kindt et al. (in prep.) →



➤ L1527 vs evolved disks



Abundances (w.r.t. C18O) in evolved disks taken from :

- Öberg, K. I.; Facchini, S.; Anderson, D. E. Protoplanetary Disk Chemistry. *Annu. Rev. Astron. Astrophys.* **2023**, *61*, 287–328.

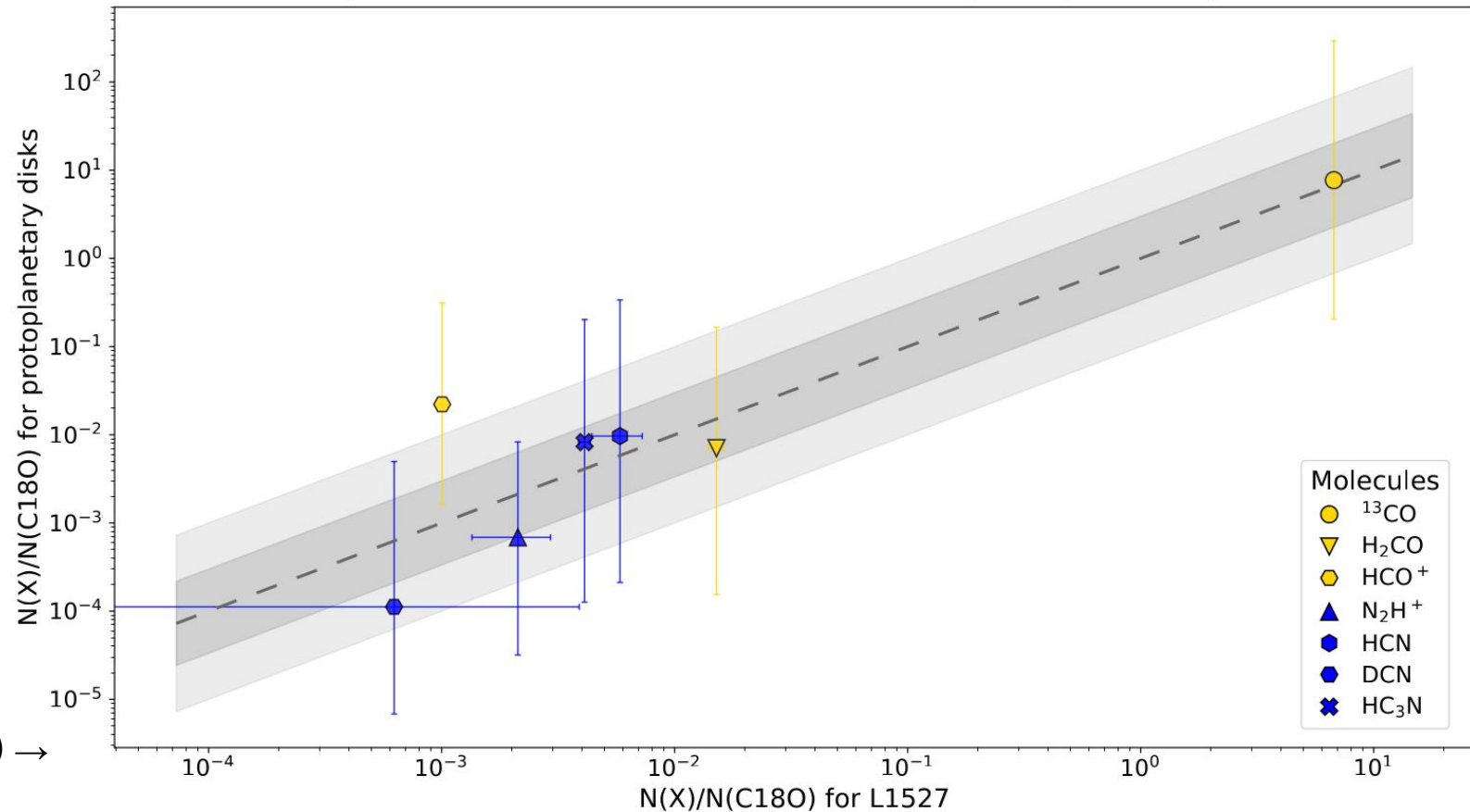
They use data from 14 different papers to get the distribution of column densities in 28 evolved disks

- Mostly around T Tauri stars
- Different SFR

Wide distribution of N_{tot}

- Precise values not specified in Öberg et al. (2023)

Comparison of abundances in L1527 and protoplanetary disks



T'Kindt et al. (in prep.) →

➤ Conclusions & perspectives

- 1) More unbiased spectral survey are needed to assess if there is chemical inheritance from the envelope

Other Class 0 and Class I protostars need to be targeted

- 2) An automatic tool is needed to analyse these kind of datasets

The MCMC and LTE tools will be extended to whole maps

- 3) Few changes in chemical abundances are seen at the large scales of L1527

1mm observations will improve the chemical inventory and provide higher angular resolution observations

- 4) More molecular abundances are needed in more protoplanetary disks

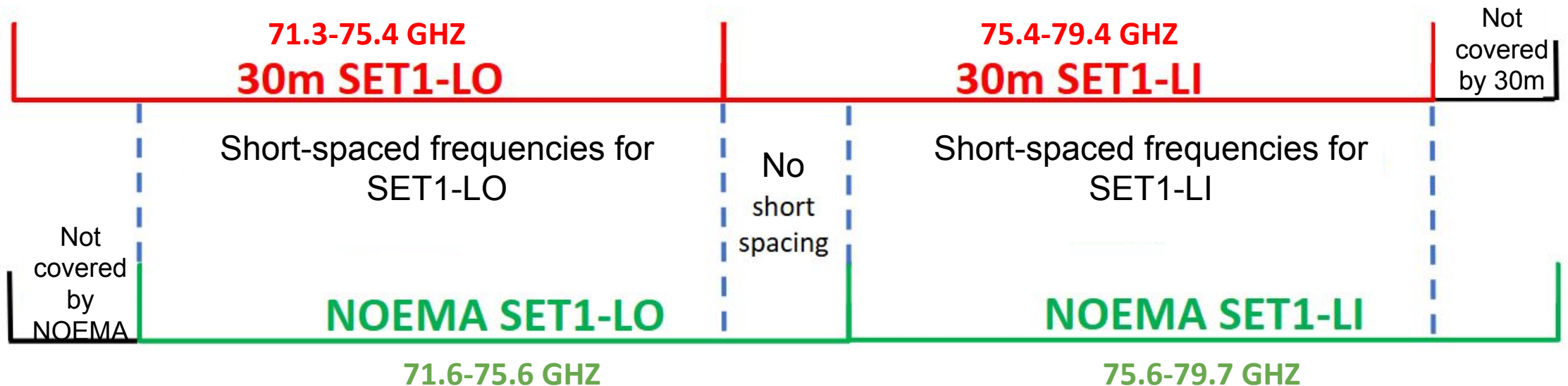
DiskStrat ALMA large program will help improve this statistic



APPENDICES :

➤ Appendix: Merging of IRAM 30m and NOEMA datasets

- Band of 40 GHz (from ~71 GHz to ~111 GHz ; 3 setups of 4 subbands each)
- Short-spacings are necessary to retrieve extended emission
- NOEMA and 30m bands are not perfectly aligned

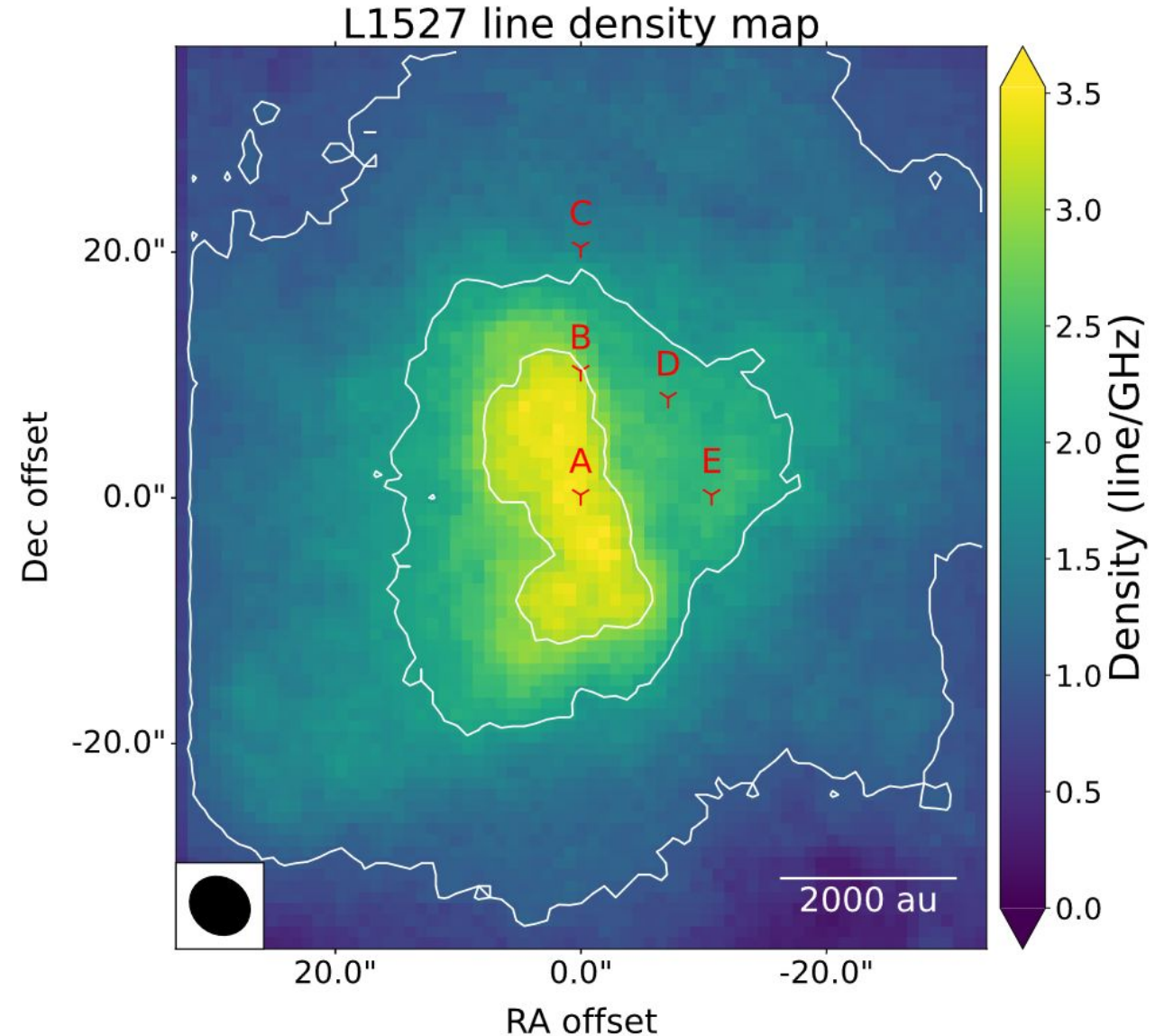


➤ Line density map

More lines toward the centre of L1527
→ Not necessarily a direct change in chemical composition

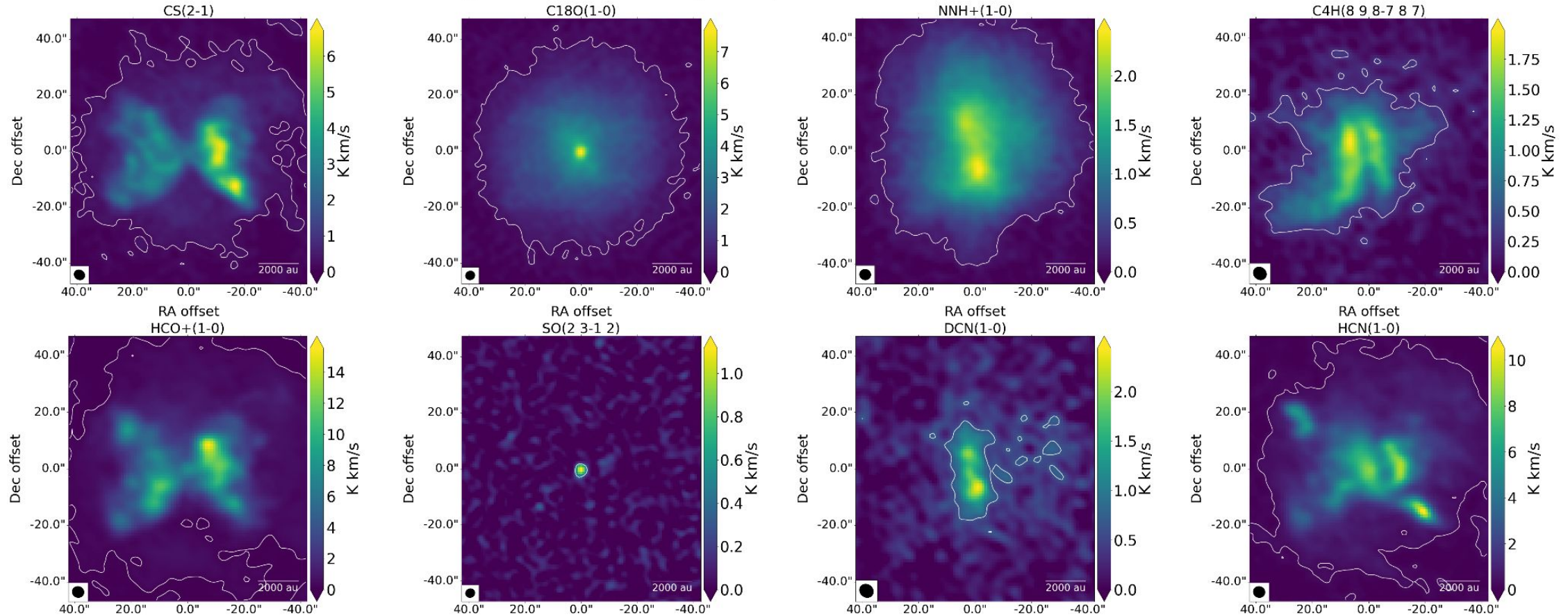
Line from carbon chains represent :

- 71.8% of total lines at A
- 75.2% of total lines at B
- 63.5% of total lines at C
- 70.0% of total lines at D
- 68.4% of total lines at E



Density of lines with a peak intensity above 5 times the noise in L1527.

➤ Moment 0 maps



Classify the molecules depending on their spatial extension and compare with the results from Tychoniec, Ł.; Van Dishoeck, E. F.; Van 'T Hoff, M. L. R.; Van Gelder, M. L.; Tabone, B.; Chen, Y.; Harsono, D.; Hull, C. L. H.; Hogerheijde, M. R.; Murillo, N. M.; Tobin, J. J. *Which Molecule Traces What: Chemical Diagnostics of Protostellar Sources*. *A&A* **2021**, 655, A65.



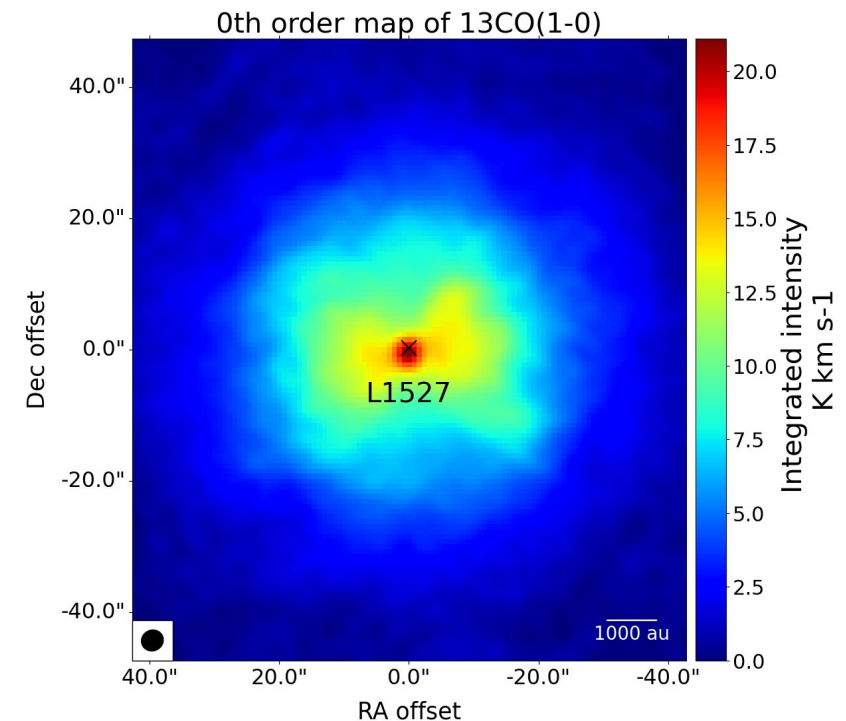
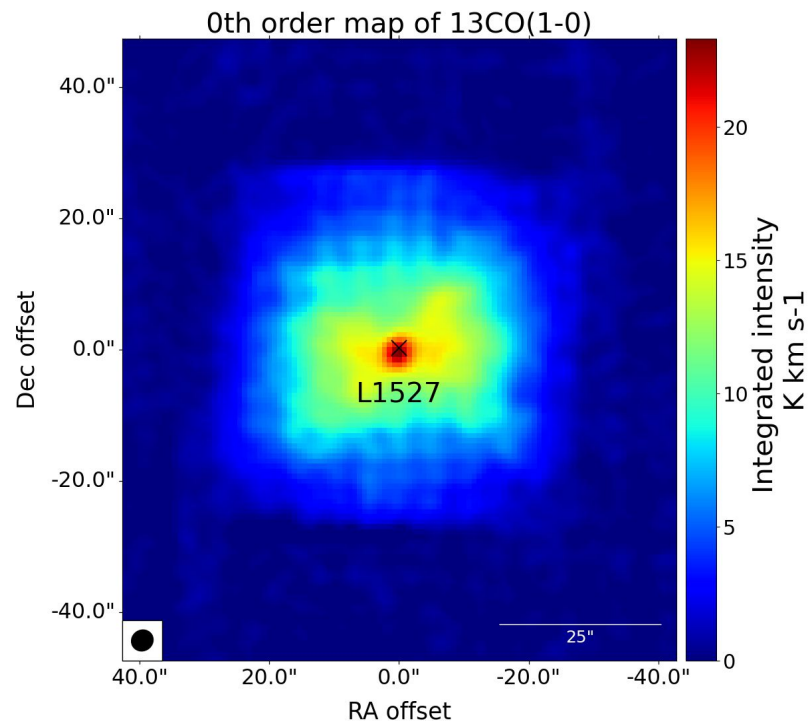
Appendix: Imaging of merged data : HOGBOM or MRC ?

HOGBOM:

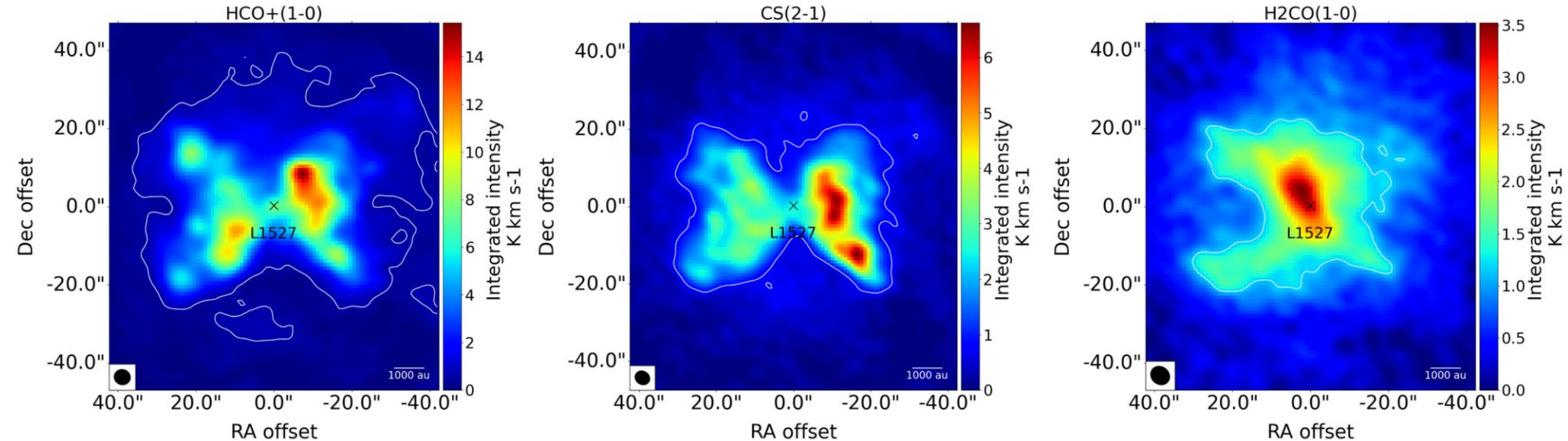
- Most common and robust one
- Clean highest intensity component
- Adds is to clean component table
- Can produce poor results on extended structures
- Grid pattern might originates from On-the-fly observation with 30m

MRC:

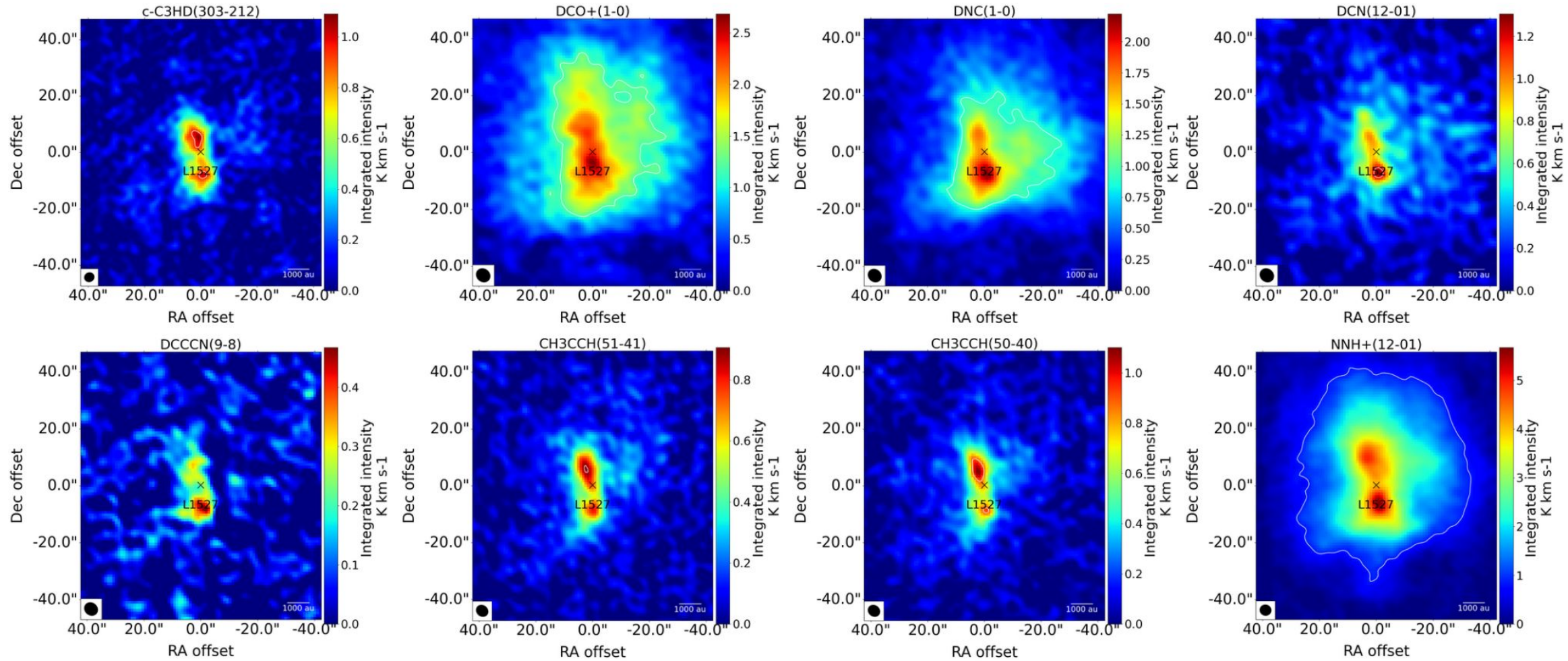
- Uses two intermediate maps
- Smoothed one for improved results on extended structures
- Difference one for spatial resolution
- Gets rid of grid pattern



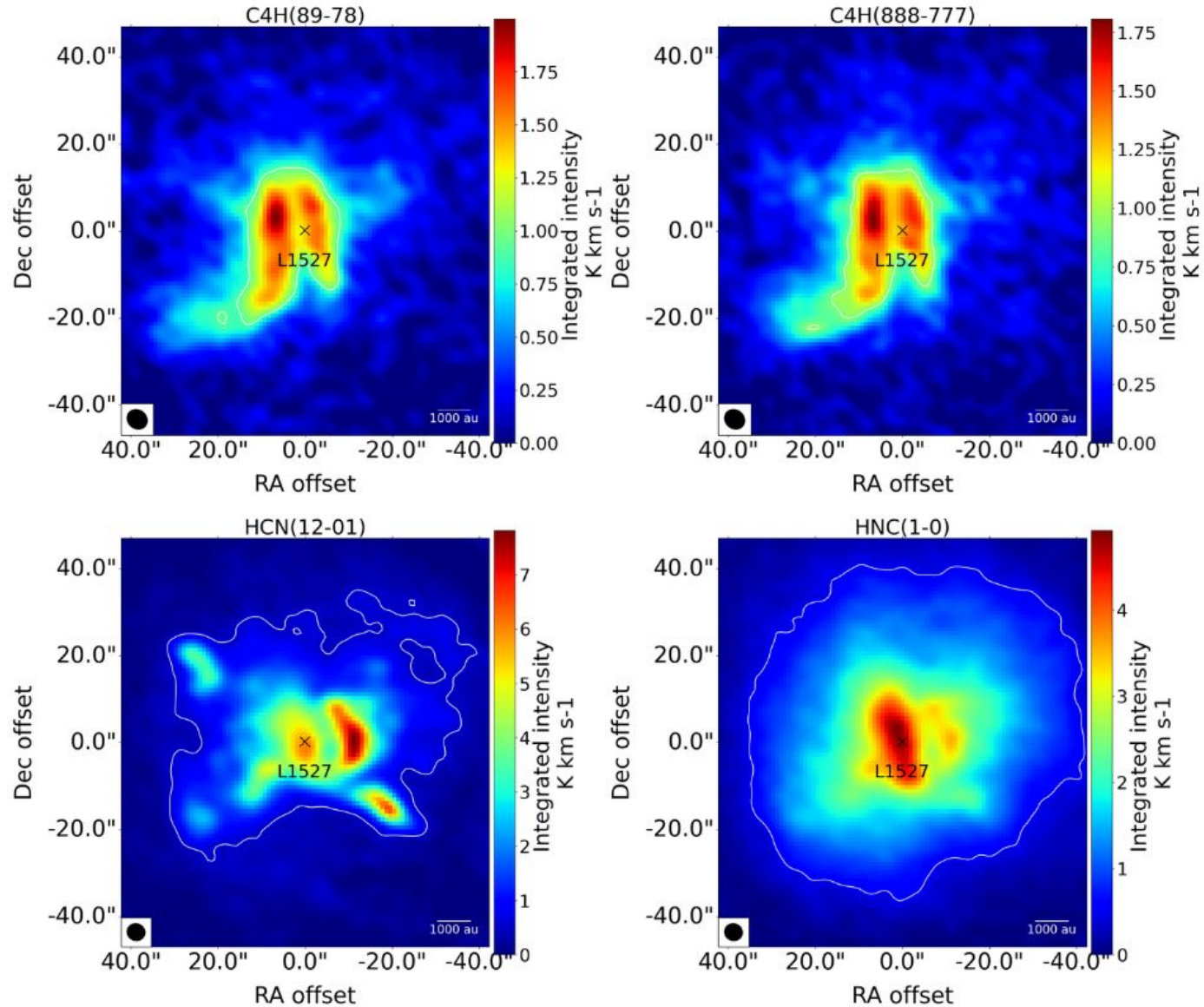
➤ Appendix: Base of cavities emission



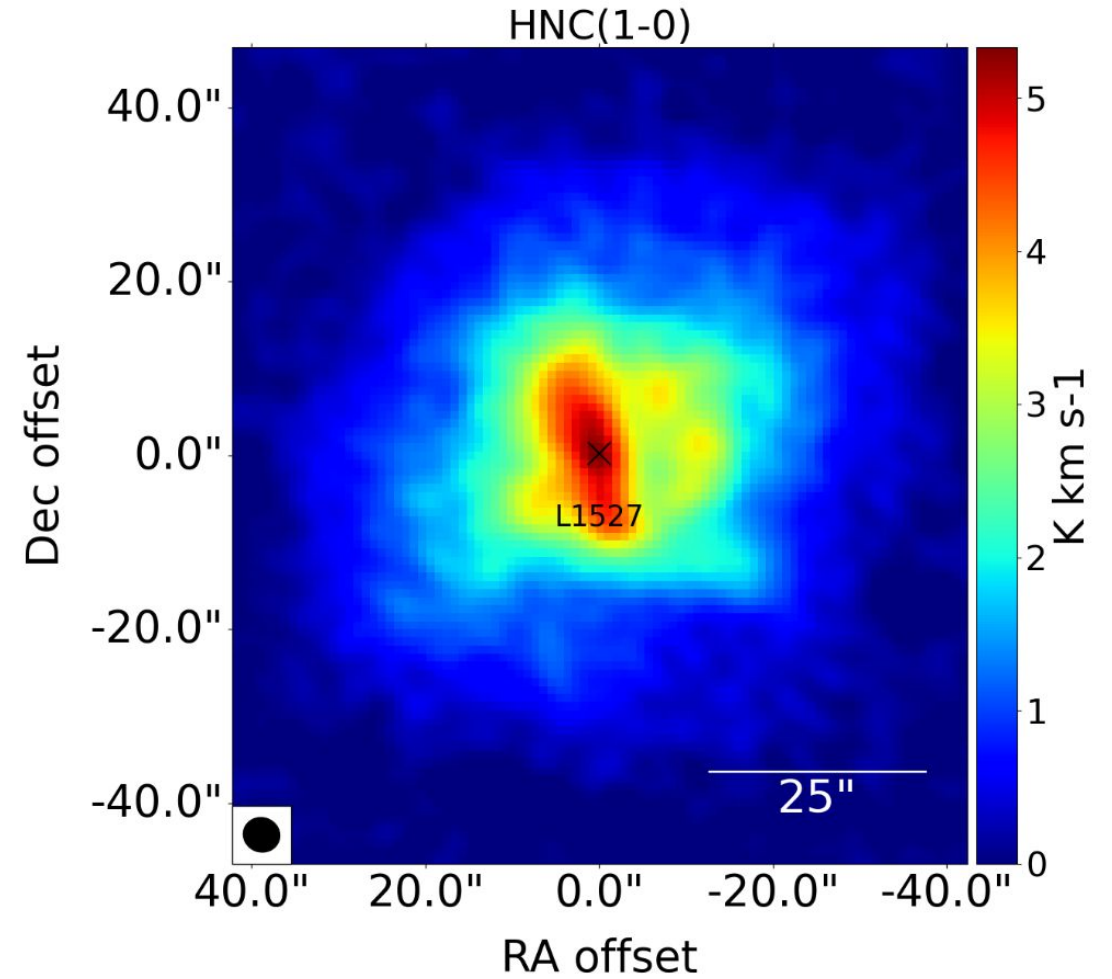
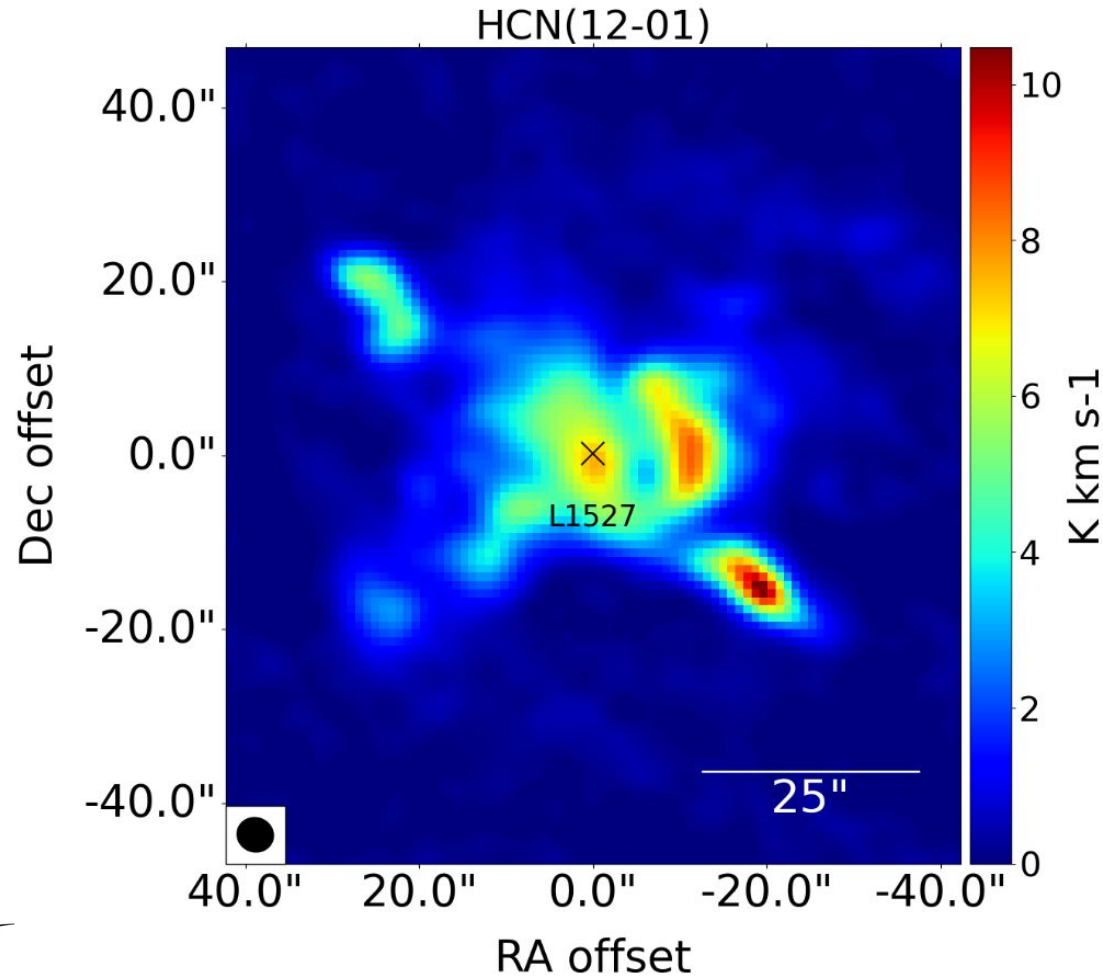
Appendix: North-South emission



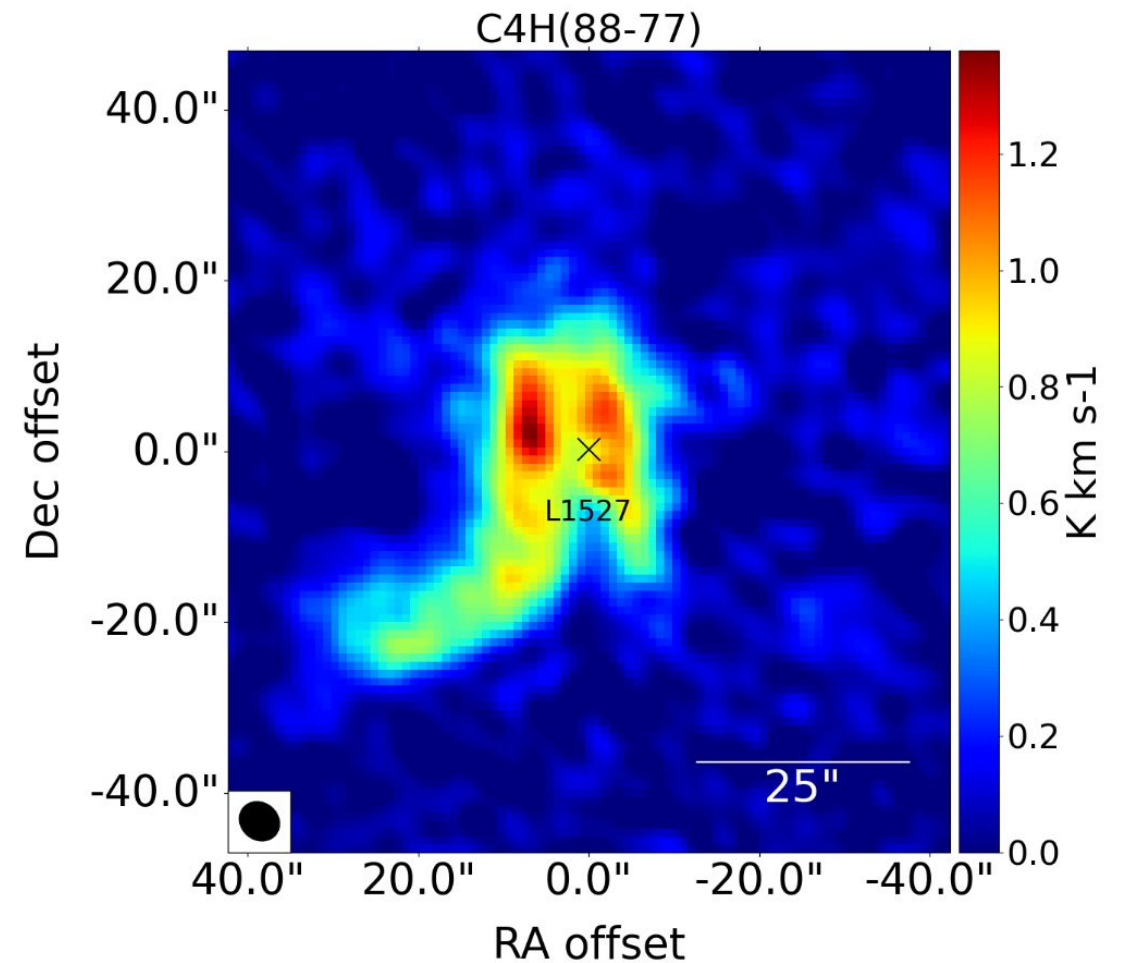
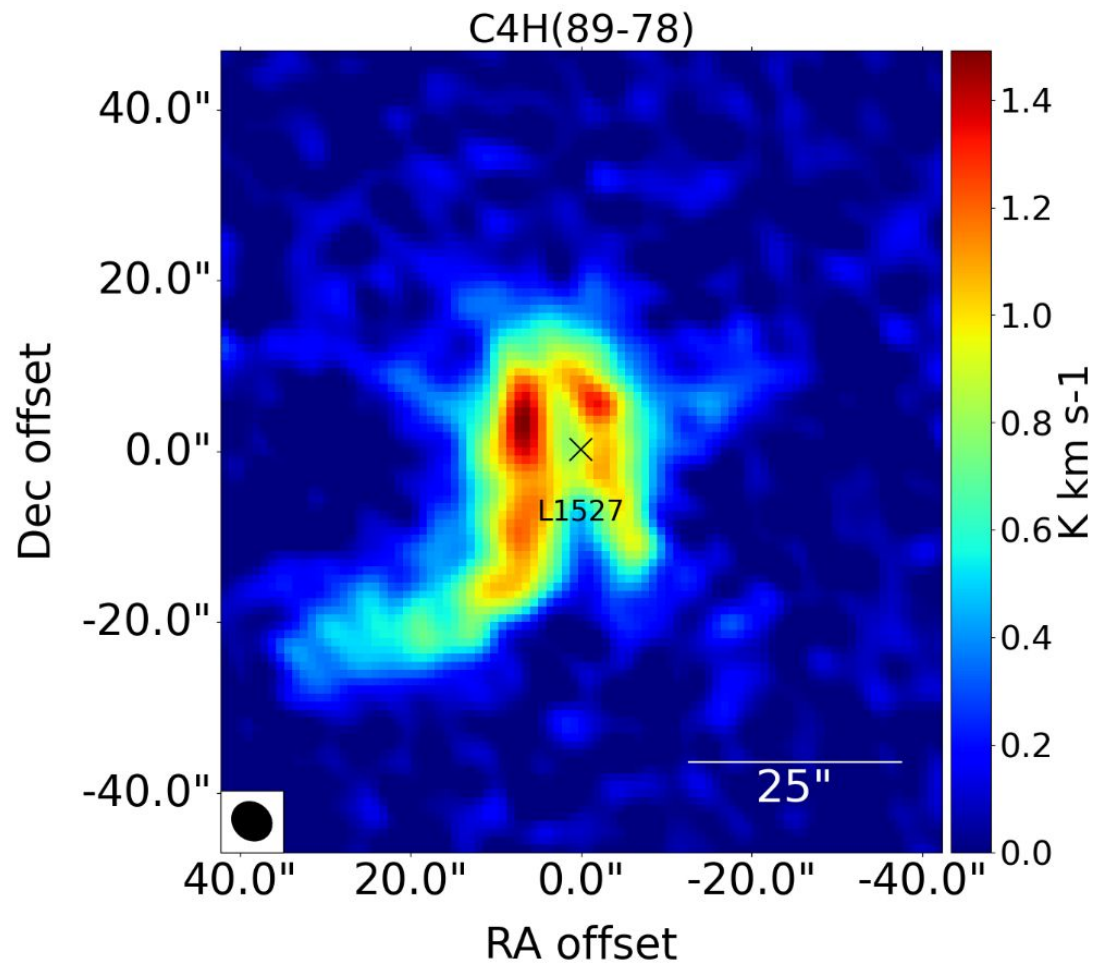
➤ Appendix: Not fully understood emission :



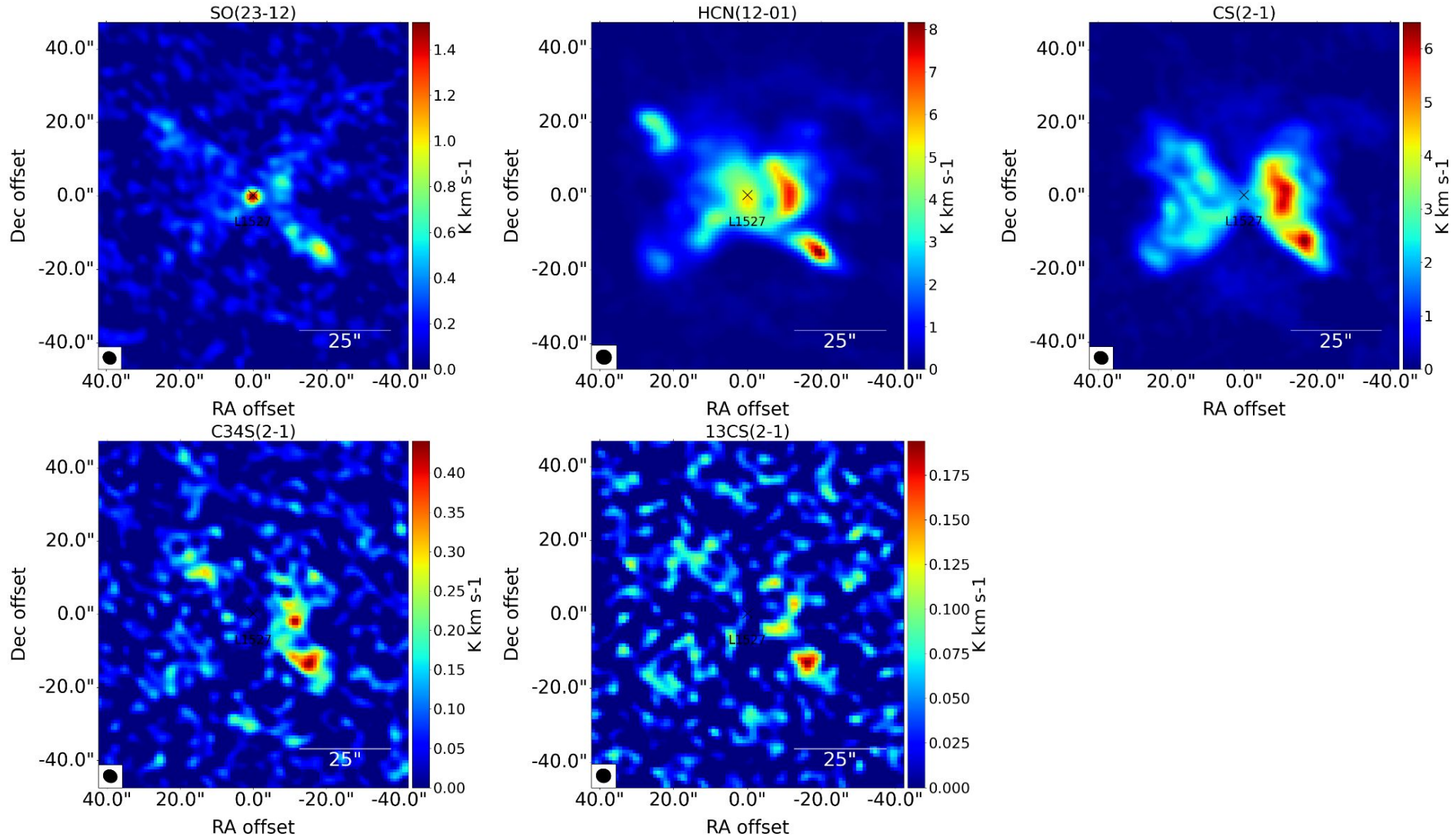
➤ Appendix : «loop» emission



➤ Appendix : «Coma» emission



➤ Appendix : South-West emission



➤ LTE line fitting hypothesis

Uniform medium along all lines of sight (LoS)

- Not true everywhere
- Seen, for example, with doubly peaked molecules in the cavities

Optically thin lines

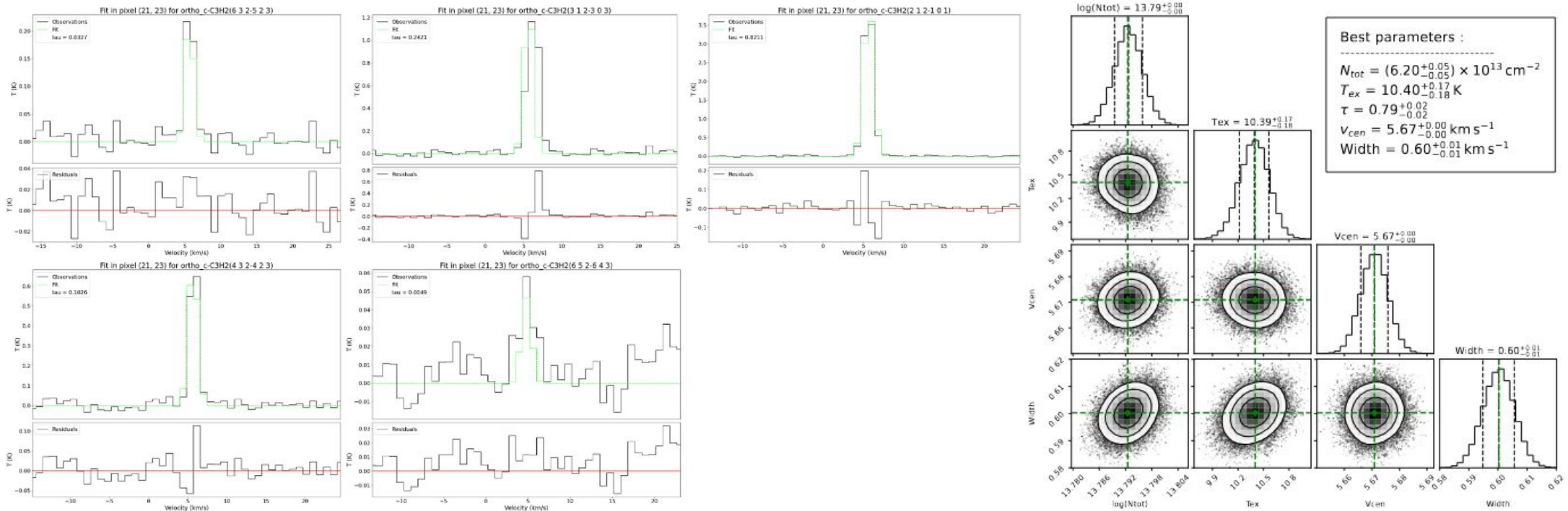
- Not the case for the LoS passing through the EoD

Local Thermodynamical Equilibrium

- Might not hold everywhere
- LTE vs non-LTE regions changes for each molecule (different critical densities)

➤ LTE line fitting method

Using a coupling between Markov Chain Monte Carlo (MCMC) and LTE line modeling tools (for rotational and hyperfine lines)



Example of MCMC + PySpecKit outputs. **Left:** Best fit VS observations and residuals. **Right:** Corner plots with the posterior distribution and best fit parameters

➤ Tobin et al. (2012) model parameters

Table 6
Model Parameters

Parameter	Description	Paper I Model	Best-fit Model	Parameter Use
R_* (R_\odot)	Stellar radius	2.09	2.09	fixed
T_* (K)	Stellar temperature	4000	4000	fixed
L_* (L_\odot)	System luminosity	2.75	2.75	fixed
M_* (M_\odot)	Stellar mass	0.5	0.19 ^a	fixed
M_{disk} (M_\odot)	Disk mass	0.005	0.0075	varied
h (100 AU)	Disk scale height at 100 AU	36.3	48.0	varied
H_0	Disk scale height at R_*	0.03	0.03	varied
p	Disk radial density exponent	3.0	2.5	varied
γ	Disk scale height exponent	1.27	1.3	varied
\dot{M}_{disk} ($M_\odot \text{ yr}^{-1}$)	Disk accretion rate	3.0×10^{-7}	1.5×10^{-6}	fixed
R_{trunc} (R_*)	Magnetosphere corotation radius	3.0	3.0	fixed
F_{spot}	Fractional area of accretion hotspot	0.01	0.01	fixed
$R_{\text{disk,min}}$ (R_*)	Disk inner radius	14.25	14.25	fixed
$R_{\text{disk,max}}/R_c$ (AU)	Disk outer radius	190	125	varied
$R_{\text{env,min}}$ (R_*)	Envelope inner radius	42.75	42.75	fixed
$R_{\text{env,max}}$ (AU)	Envelope outer radius	15,000	15,000	fixed
\dot{M}_{env} ($M_\odot \text{ yr}^{-1}$)	Envelope mass infall rate	0.8×10^{-5}	4.5×10^{-6a}	fixed
$\rho_{1 \text{ AU}}$ (g cm^{-3})	Envelope density at 1 AU	5.8×10^{-14}	7.25×10^{-14}	varied
b_{out}	Outer cavity shape exponent	1.5	1.5	fixed
$\theta_{\text{open,out}}$ ($^\circ$)	Outer cavity opening angle	20	20	fixed
θ_{inc} ($^\circ$)	Inclination angle	85	85	fixed
ρ_c (g cm^{-3})	Cavity density	0	0	fixed
$\beta_{\text{dust, millimeter}}$	Millimeter dust spectral index	...	0.25	varied

Table 6. extracted from the paper of Tobin et al. (2012) showing the parameters used in their model of L1527

➤ Calculation of the abundances

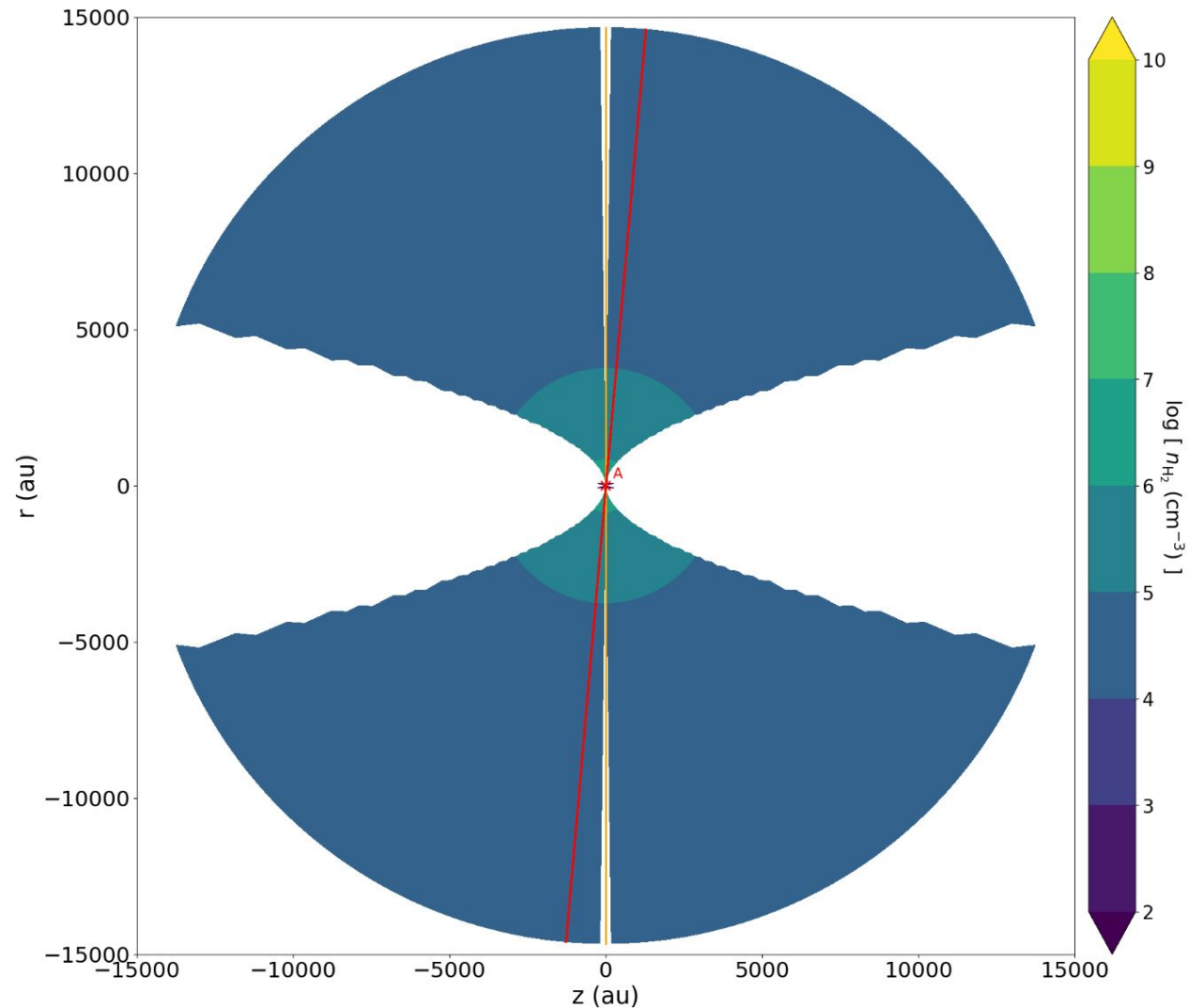
$n(\text{H}_2)$ model of L1527 done by Tobin et al. (2012)

- Based on a classic collapsing envelope density model (Ulrich 1976 ; Cassen & Moosman 1981 ; Terebey et al. 1984)

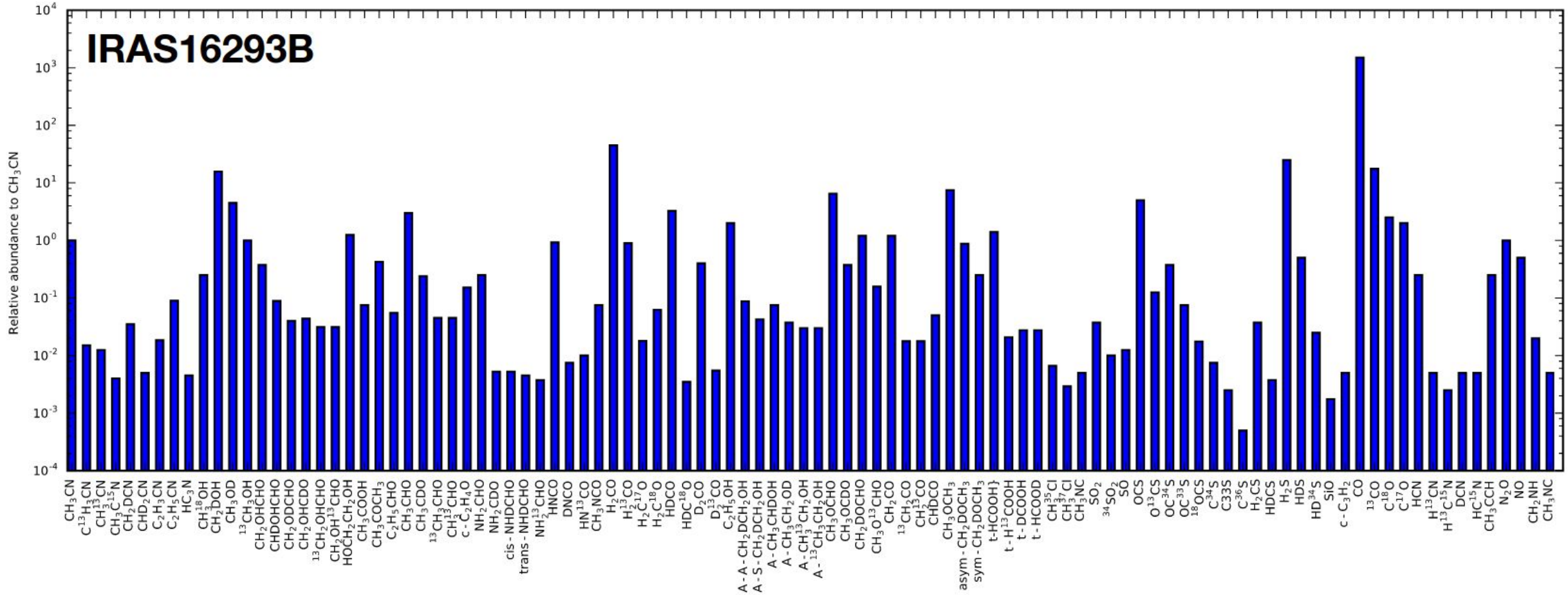
Calculations of the lines of sight (LoS) for the five selection position

For position A :

- Opacity effect from the disk → Emission seen only from the foreground
- Not full LoS



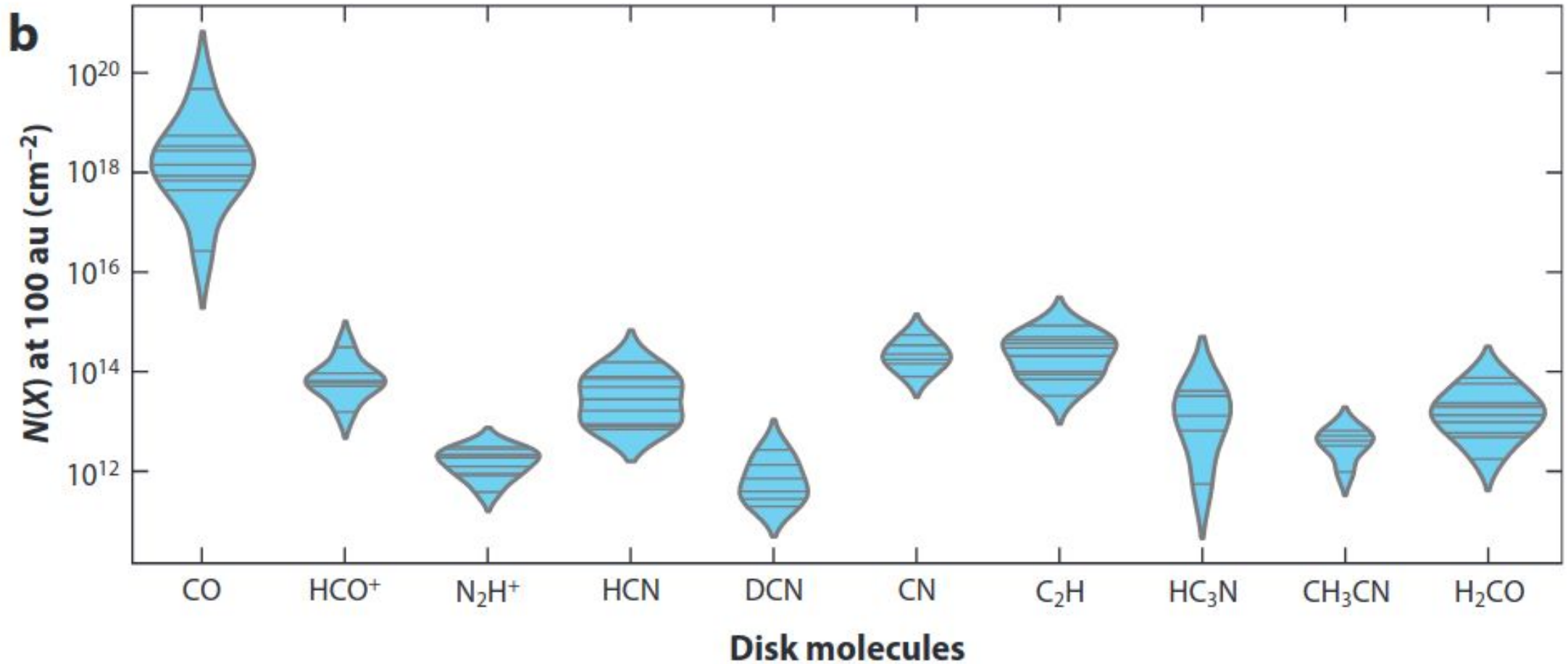
➤ Abundances (w.r.t. CH₃CN) from PILS :



Extracted from slide 16 of the Jørgensen, J. Exploring the Complex Chemistry of Embedded Protostars. presentation for the International symposium on molecular spectroscopy (2019)

Show the abundances in IRAS 16293 B w.r.t. the one of CH₃CN obtained in the different papers from PILS

➤ Sources used in Obérg et al. (2023)



Extracted from Fig. 4 (panel b) of the paper

Show the outer disk column densities from ALAM observations. The width of the distributions correspond to the number of disks that fall within that column density. Each of the line shows an individual measurement.

➤ Sources used in Obërg et al. (2023)

<u>Name :</u>	<u>Type/Age :</u>	<u>Position/SFR :</u>	<u>Ref :</u>
HD 163296	Herbig Ae	---	1 ; 4 ; 5 ; 6 ; 7 ; 8 ; 9 ; 11
TW Hya	T Tauri	Hydra	2 ; 7 ; 12 ; 14
LkCa 15	T Tauri	Taurus	3 ; 5
GM Aurigae	T Tauri	Taurus-Auriga	3 ; 6 ; 8 ; 9 ; 11
DM Tau	T Tauri	Taurus	3 ; 5 ; 7
V4046 Sgr	K-type main sequence	Sagittarius	3 ; 5
AS 209	T Tauri	Ophiuchus	3 ; 4 ; 5 ; 6 ; 8 ; 9 ; 11
IM Lup	YSO T Tauri Class II	Lupus	3 ; 4 ; 5 ; 6 ; 7 ; 8 ; 9 ; 11
Elias 24	T Tauri	Ophiuchus	4
Elias 27	Class II YSO	Ophiuchus	4
GW Lup	T Tauri	Lupus	4
HD 142666	T Tauri	Ophiuchus	4
HD 143006	T Tauri	Upper Sco	4 ; 5
Elias 20	T Tauri	Ophiuchus	4

➤ Sources used in Obërg et al. (2023)

<u>Name :</u>	<u>Type/Age :</u>	<u>Position/SFR :</u>	<u>Ref :</u>
RU Lup	T Tauri	Lupus	4
Sz 114	T Tauri	Lupus	4
Sz 129	T Tauri	Lupus	4
CI Tau	T Tauri	Taurus	5
DO Tau	T Tauri	Taurus	5
J1604-2130	Dipper/AA Tau	Upper Sco	5
J1609-1908	T Tauri	Upper Sco	5
J1612-1859	T Tauri	Ophiuchus (??)	5
J1614-1906	T Tauri	Upper Sco	5
MWC 480/HD 31648	Herbig AeBe	Taurus-Auriga	5 ; 6 ; 8 ; 9
PDS 70	~5 Myr T Tauri	Centaurus	10 ; 11
SR 4	T Tauri	Ophiuchus	4
DoAr 25	T Tauri	Ophiuchus	4
GG Tau	Triple T Tauri	Taurus-Auriga	13

➤ Sources used in Obërg et al. (2023)

- 1) Qi et al. (2011)
- 2) Qi et al. (2013)
- 3) Qi et al. (2019)
- 4) S. Zhang et al. (2018)
- 5) Bergner et al. (2019)
- 6) Bergner et al. (2021)
- 7) K. Zhang et al. (2019)
- 8) K. Zhang et al. (2021)
- 9) Cataldi et al. (2021)
- 10) Facchini et al. (2021)
- 11) Guzman et al. (2021)
- 12) Öberg et al. (2021a)
- 13) Phuong et al. (2021)
- 14) Terwisscha van Scheltinga et al. (2021)